Letters in Applied NanoBioScience
Open-Access Journal (ISSN: 2284-6808)

Article
Volume 13, Issue 4, 2024, 182
https://doi.org/10.33263/LIANBS134.182

Analyzing Intrinsic Molecular Dynamics in Alkyl Azoxybenzene Compounds using Functional Data Analysis for Intermolecular Potentials and the Odd-Even Effect

Mahadevanna Sushma[1], Jademadegowda Mahadeva[2,*], Manju Varanchi Venkata Shetty [3,*], Nandaprakash Mysore Basavaraju [4], Vinayakaprasanna N Hegde [3], Somashekar Rudrappa [5]

1 Department of Physics, Yuvaraja's College, University of Mysore, Mysuru, India – 570005
2 Department of Physics, PES College of Science, Arts and Commerce affiliated to University of Mysuru, PET Research Foundation, Mandya, India – 571402
3 Department of Physics, Vidyavardhaka College of Engineering (Affiliated to VTU, Belagavi), Mysuru, India – 570002
4 Department of Physics, Karnataka State Open University, Mukthagangothri, Mysuru, India – 570006
5 Regional Institute of Education and Center for Material Science, Vijnana Bhavan, Manasagangotri, University of Mysore, Mysuru, India – 570017
* Correspondence manjuvv@vvce.ac.in (M.V.V) & jmahadeva@yahoo.com (J. M);

Scopus Author ID: 57194472856
Received: 2.08.2023; Accepted: 8.07.2024; Published: 28.08.2024

Abstract: Computational modeling has provided a comprehensive understanding of a series of liquid crystalline materials. The findings were additionally compared to the experimental values reported for certain compounds in the series. The research simulates various physical properties such as transition temperature, order parameter, Van der Waals potential, pair energy, specific heat, and pair correlation function. Examining these properties aims to comprehend the importance of carbon atoms and their interactions, both within and between molecules, which ultimately contribute to the manifestation of mesophase behavior. This study utilizes the molecular dynamics method as a means to explore the liquid crystalline properties. The primary objective is to uncover the range and nature of the mesophase exhibited by these compounds. The results obtained thus far strongly support this research direction, and knowledge of these compounds finds applications in sensitive nucleic acid detection, label-free protein analysis, and the development of biocompatible sensors for real-time cellular monitoring.

Keywords: liquid crystals; LAMMPS; FDA; mesophase; lattice energy.

1. Introduction

Liquid crystals, discovered in the 19th century, have fascinated researchers, leading to extensive scientific exploration into the mechanisms underlying the mesophase phenomenon. [1-4]. The mesophase can be observed through temperature changes (thermotropic phase) and variations in solvent, adding to its intrigue [5]. Liquid crystals manifest in diverse realms, including plants, DNA molecules, cellulose, and other life science materials, showcasing their widespread presence in nature. Particularly noteworthy are certain mesogenic organic compounds that play a vital role in liquid crystalline displays (LCD) commonly encountered in everyday life [6]. Their essential application in LCD technology underscores the practical significance of studying liquid crystals [7-11]. Luckhurst's work on intermolecular forces in liquid crystals provides valuable insights into the molecular theories of Nematics [12], particularly focusing on long-range anisotropic intermolecular potentials. This research is

instrumental in understanding liquid crystals' fundamental behavior and properties. Monte Carlo simulations [13] have emerged as a powerful tool for studying phase transitions in confined mesogenic fluids, offering significant insights into how liquid crystals behave under constrained movement and in diverse environments [14]. Molecular dynamic calculations have also been crucial in determining the Frank elastic constants in nematic liquid crystals, providing essential information about their mechanical properties and behavior. In another notable study, molecular simulations have been utilized to explore the complex interactions between nanoparticles and liquid crystals [15], specifically investigating the entangled defect structures that form around nanoparticles in nematic liquid crystals [16,17]. This research deepens our understanding of these interactions, with potential applications in areas like nanotechnology and materials science. The ongoing advancements in liquid crystal research promise exciting developments and applications in various fields [18-19], making it an intriguing time to delve into the world of liquid crystals. The following materials have been considered for these investigations [20-21]. The structural composition of Alkyl Azoxybenzenes is shown in Figure 1.

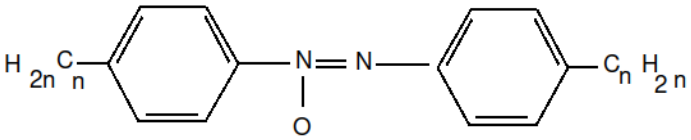

Figure 1. Structural Composition of Alkyl Azoxybenzenes.

p-azoxybenzene (n=0), No mesophase and crystal structure data has been reported [21], 4,4`-di-2-alkyl azoxy benzenez (n=2), Cryst-nematic (18°C), Nematic- ISO (27°C), 4, 4`-di-3-alkyl azoxy benzene (n=3), Nematic- ISO (60°C), 4, 4`-di-4-alkyl azoxy benzene (n=4), Cryst-nematic (18°C), Nematic-ISO, (27°C), 4, 4`-di-5-alkyl azoxy benzene (n=5), Cryst-nematic (22°C) Nematic – ISO, (72°C, MP 18°C), 4, 4`-di-6-alkyl azoxybenzene (n=6), Cryst-nematic (21°C) Nematic- ISO, 49°C, MP 22°C, MP), 4, 4`-di-7alkyl azoxy benzene (n=7). Cryst-nematic (34.5°C) Nematic ISO, 71°C, MP 21°C.

The study aims to understand why some compounds in a homologous series exhibit mesophase while others do not. By analyzing intra and intermolecular potentials alongside order parameters, we aim to uncover the reasons for this variability in mesophase behavior. Additionally, we are interested in exploring the diversity of mesophases observed within the series. This involves examining potential energy contributions from different bond lengths, angles, and dihedral distributions. Ultimately, our goal is to identify the key parameters influencing mesophase behavior in these compounds, leading to valuable insights into their fundamental properties.

2. Materials and Methods

The investigation involved molecular systems with a significant number of atoms using the Dreiding potential for the united atom model and the interatomic force field. The strain rates varied widely, enabling a thorough exploration of molecular behavior under different conditions [22-24]. The LigParGen website by the Jorgensen group was utilized for this research, providing tailored force field parameters for organic molecules [25-27]. The simulations were performed using LAMMPS with an optimized input script for efficiency and parallelization, ensuring effective simulations of molecular systems. The simulations spanned temperatures from 300 to 600 K, exploring properties and behavior across different thermal

conditions. Microstructure metrics such as bond lengths, angles, and dihedral angles were calculated, offering insights into molecular structure and conformational changes. Thermodynamic properties like total energy, pressure, volume, density, enthalpy, and Van der Waals energy were monitored as functions of temperature, providing valuable information about system behavior, stability, and intermolecular interactions. In summary, combining the united atom model, interatomic force field, LigParGen, LAMMPS simulations [28], and the analysis of microstructure metrics and thermodynamic properties offers a robust framework for investigating the molecular systems under examination.

3. Results and Discussion

3.1. Stress-strain-behavior.

The stress-strain behavior is pivotal in materials demonstrating a mesophase [25,29,30]. In this study, we have plotted the isothermal stress-strain curves at 100 K, utilizing a strain rate of 10^{10} s^{-1}, for all seven members of the homologous series. Figure 2 displays these curves. For a deeper dive into the computational aspects, the LAMMPS manual offers valuable guidance. The flowchart of our simulations, depicted in Flowchart 1, serves as a helpful visual depiction of the workflow and stages encompassed in our research.

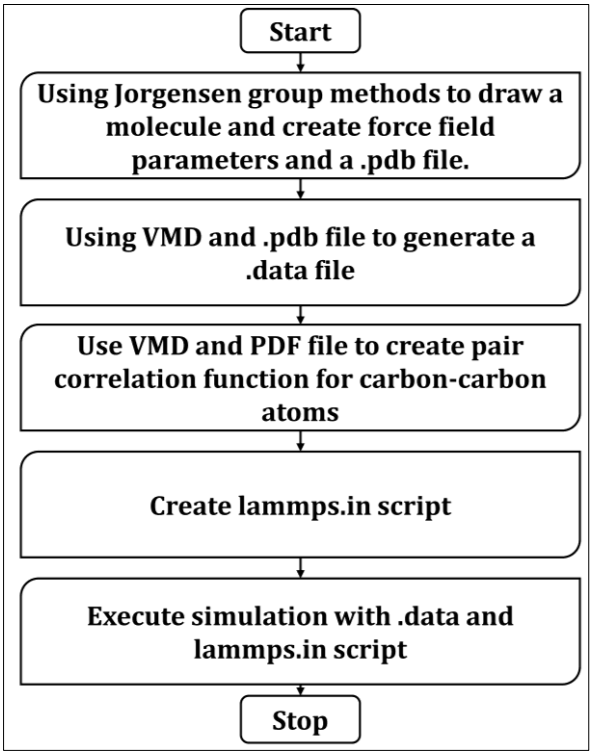

Flowchart 1. Flowchart for simulation of organic molecules.

The stress-strain curve displays a single regime of elasticity followed by a decrease, indicating a softening behavior like observations in various polymers [24, 29]. As the chain length increases, there is a general decrease in stress/strain values, although it alternates with several carbon atoms for each stress/strain ratio. These oscillations arise due to minor temperature fluctuations, approximately 10 percent of the mean value. These findings enhance our understanding of the relationship between structure and mechanical behavior in materials exhibiting a mesophase.

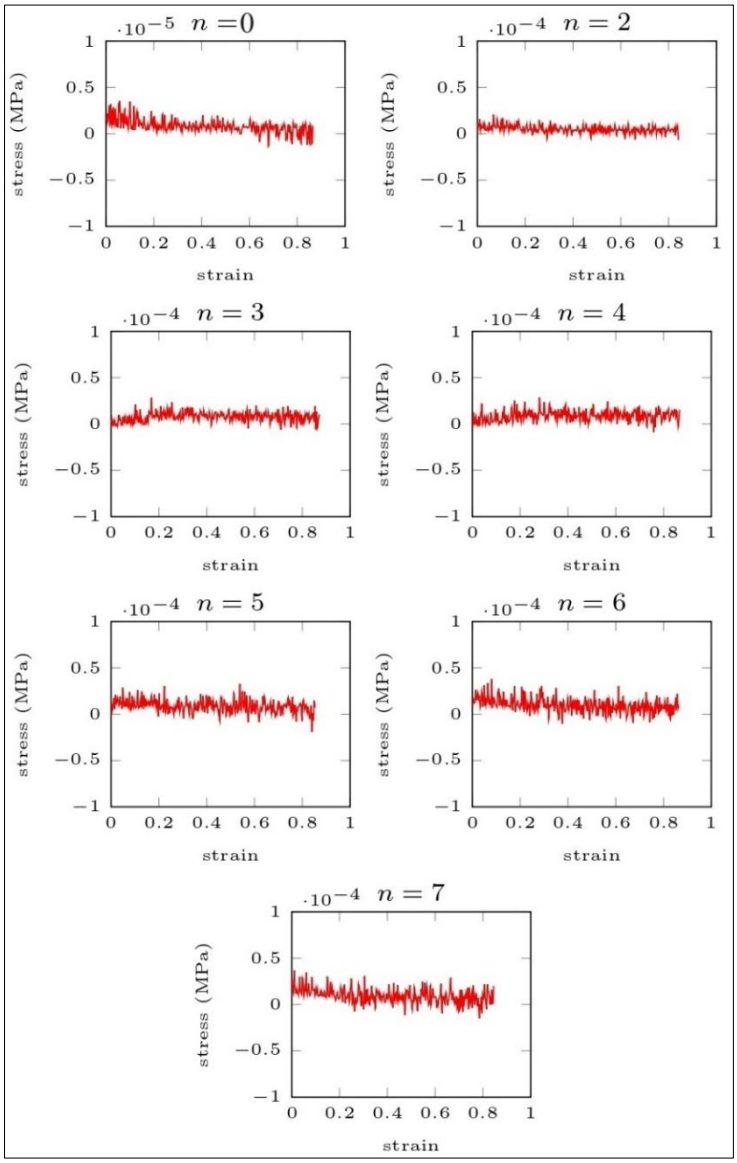

Figure 2. Stress-strain behavior in seven compounds of homologous series.

3.2. Pair distribution function.

The Pair Distribution function (PDF) is normally given by

$$g(r) = \frac{1}{\rho}\frac{dn(r,r+dr)}{dv(r,r+dr)} \quad (1)$$

In this study, we used the radial distribution function (RDF) to analyze particle distribution around a selected molecule. The RDF results obtained at room temperature (300 K), depicted in Figure 3, show peaks corresponding to different shells of neighboring particles. Notably, the first peak in the RDF curve signifies the number density of the first nearest neighbors, indicating closely positioned neighboring particles around the chosen molecule. Additionally, the extended ordering up to third-order nearest neighbors is influenced by inter- and intra-molecular interactions, offering valuable insights into particle arrangement within the homologous series.

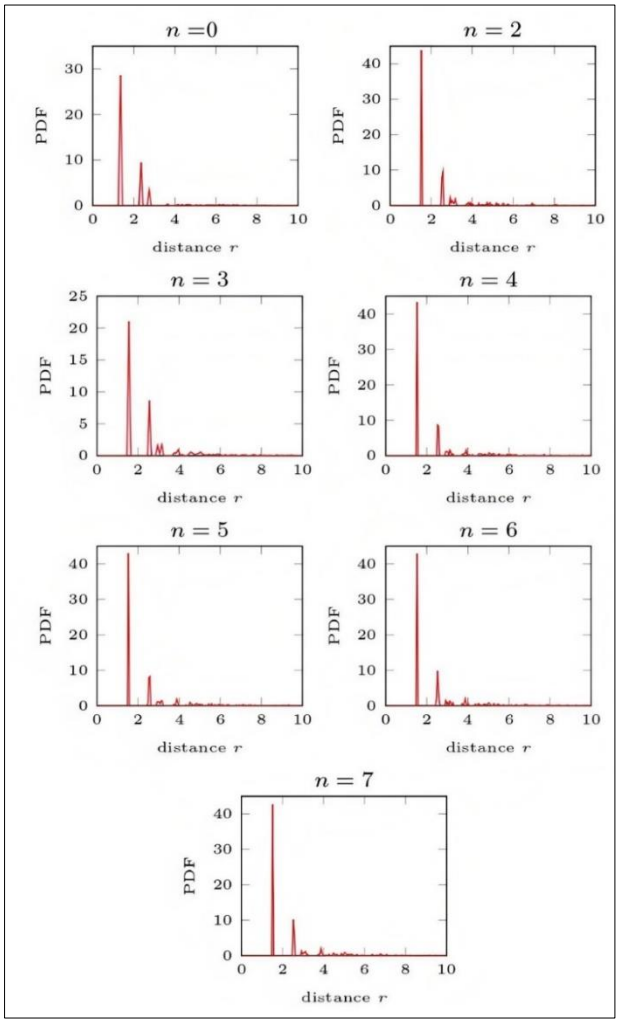

Figure 3. Pair distribution function in seven compounds of homologous series.

3.3. Total lattice energy and order parameter variation with temperature.

In this investigation, we computed the order parameter, total energy, bonding energy, bond angle energy, and dihedral energy across various temperature ranges. Figure 4 comprehensively compares these energies between n = 0 and n = 7 in the homologous series.

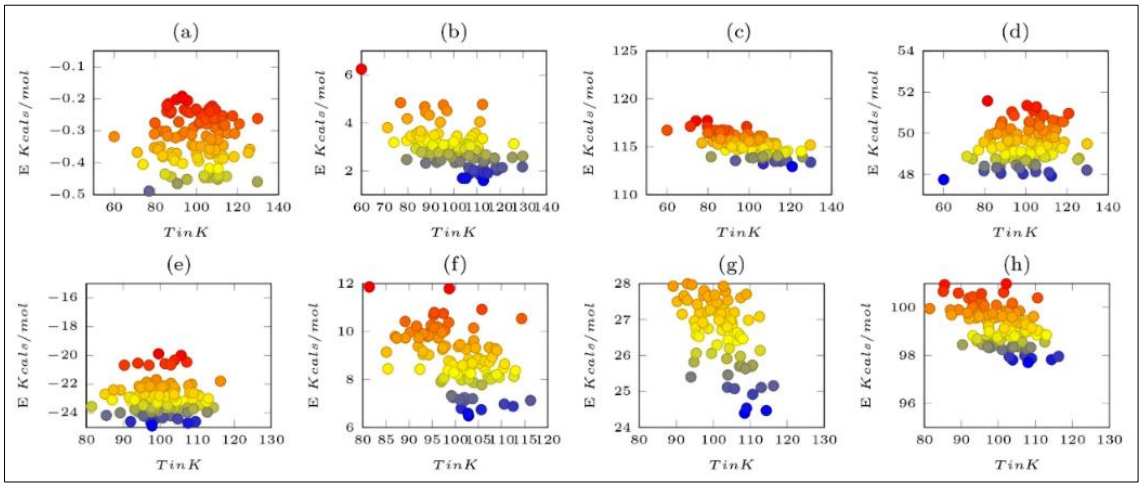

Figure 4. For n=0, **(a)** pair energy; **(b)** bond energy; **(c)** angle energy; **(d)** dihedral energy and n=7; **(e)** pair energy; **(f)** bond energy; **(g)** angle energy; **(h)** dihedral energy computed. Colors indicate higher and lower values.

It's intriguing to note a gradual increase in all energies as the number of carbon atoms in the end chain increases on either side of the bridge group. This suggests that bonding, bond angles, and dihedral angles contribute more energy as the carbon chain lengthens. Particularly significant changes are observed in dihedral energy as the chain length increases, highlighting the crucial role of dihedral angles in determining system energy.

Statistically, one can define the orientational order parameter as

$$\overline{P}2 = \frac{1}{2}\frac{\int_{-1}^{+1}[3x^2-1]P(x)dx}{\int_{-1}^{+1}P(x)dx} \qquad (2)$$

The distribution function P(x), where x = cos θ, quantitatively describes the orientation of molecules in a liquid crystalline phase within a specified volume [30-32]. In a nematic phase characterized by perfect alignment along specific directions, the measure attains a value of one, contrasting with the isotropic phase, where it equals zero. Following P.G. de Gennes and a corresponding theoretical model [31,32], the higher-order parameter is expressed as:

$$\overline{P}4 = \frac{1}{8}\frac{\int_{-1}^{+1}[34x^4-30x^2+3]P(x)dx}{\int_{-1}^{+1}P(x)dx} \qquad (3)$$

The equations provided are,

$$P(x) = e^{\frac{ETx}{kT}} \ (4)$$

Here ET denotes lattice energy, which is determined using LAMMPS [33,34].

Moreover, these energy variations are influenced by temperature, with noticeable differences at higher temperatures. Notably, the absence of a decrease in dihedral energy at 250 K indicates a single coupled deformation mode in this system. This insight provides valuable information on deformation modes and associated energy changes in the molecules of the homologous series. Our study illuminates the system's underlying energy contributions and deformation behaviors by analyzing these energy components' temperature and chain length variations. These findings enhance our understanding of molecular dynamics and structural properties contributing to the mesophase in these compounds.

3.4. Heat capacity.

We determined the heat capacity by fitting a linear curve to the temperature-dependent total energy data. Table 1 showcases the resulting heat capacity values alongside other pertinent physical parameters.

Table 1. Computed heat capacity values. Cv in Kcal/mol/K; E-1: pair energy; E-2 Enthalpy; E-3: dihedral energy; M1=Mean; M2:min; M3:max; all energies are in units of Kcals/mol.

n	Cv	E-1			E-2			E-3		
		M1	M2	M3	M1	M2	M3	M1	M2	M3
0	0.11	-1.05	-2.49	0.45	222.9	151.7	340.6	49.5	47.7	51.6
2	0.24	-12.02	-22.12	-7.76	168.4	66.2	308.3	63.9	62.3	65.6
3	0.22	-42.27	-59.30	-8.28	186.6	53.7	319.1	70.1	68.7	71.5
4	0.30	-13.25	-27.56	-6.96	218.7	91.6	334.8	76.5	74.9	78.6
5	0.30	-11.91	-19.47	-6.47	230.8	84.7	374.2	83.9	82.3	85.4
6	0.42	-26.06	-60.19	-7.57	272.6	143.3	522.6	91.5	89.6	94.0
7	0.39	-15.46	-24.15	-8.47	292.3	129.5	465.8	99.2	97.7	101.1

Observing Table 1, it's clear that the heat capacity rises with an increasing number of carbon atoms, a trend mirrored in the average enthalpy and dihedral energies illustrated in Figure 5. These trends can be explained by the heightened intermolecular and intramolecular interactions that arise with longer carbon chains. These interactions lead to diverse molecular arrangements, thus contributing to the formation of various mesophases. These physical factors play a critical role in shaping the observed mesophase formations.

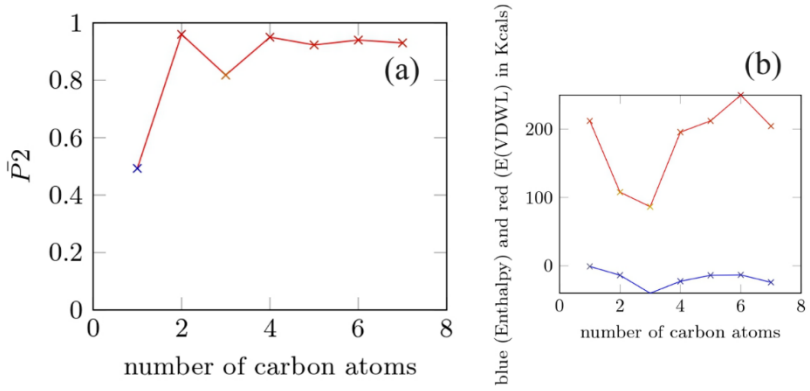

Figure 5. Variation of odd-even effect in homologous series, and variation of enthalpy and Van der Waals potential with number of carbon atoms.

3.5. Functional data analysis of parameters.

Functional Data Analysis (FDA) is a statistical branch focusing on analyzing data represented as functions or curves, first introduced by Dalzell and Ramsay in 1991. It explores the distribution of functional data, relationships between functional random variables, and more, utilizing information on derivative rates for insights [35]. FDA involves analyzing slopes, curves, and other characteristics made accessible due to inherent smoothness, aiding in multiple perspectives of data examination. Its key aspects include choosing a smoothing strategy, data reduction, grouping modification, functional linear modeling, and predictive methods. Despite the complexity often associated with functional data, FDA allows for easy identification of quantity, frequency, and trends, treating each replication as a single observation in data analysis.

Our study recognizes that quantifying correlations and dependencies between parameters may not offer a comprehensive understanding of how an increase in carbon atoms and chain length affects mesophase formation. To address this, we have implemented univariate Functional Principal Component Analysis (FPCA) [35]. Let the value of θ observed for a jth sample on the ith trial be represented as

$$\theta_{ij} = \theta_i(t_j) + \epsilon_{ij} = \mu(t_{ij}) + \sum_{k=1}^{\infty} \xi_{ik}\, \Phi_k(t_{ij}) + \epsilon_{ij}$$
$$\approx \mu(t_{ij}) + \sum_{k=1}^{M} \xi_{ik}\, \Phi_k(t_{ij}) + \epsilon_{ij} \quad (5)$$

Where ϵ_{ij} are random experimental errors. The mean function for the parameter is then estimated by solving the optimization problem.

$$\hat{\mu}(t) := \operatorname{argmin}_{f \in F} \sum_{i=1}^{n} \sum_{j=1}^{n_i} (\theta_{ij} - f(t_{ij}))^2 + \lambda \int_{\mathbb{R}\geq 0} (f''(t))^2 dt, \quad (6)$$

Our data analysis specifically considers the orientational order and total energy at the reported experimental transition temperature [36]. This approach allows us to observe

correlations among homologous members and within the parameters. To visually represent these correlations, Figure 6 showcases correlation surfaces and mean value functions for the order parameter and pair energy parameters [37]. These correlation surfaces signify the existence of multiple principal components and correlations among the parameters. Understanding these correlations is crucial as it offers insights into the interplay between different parameters and their collective impact on mesophase formation.

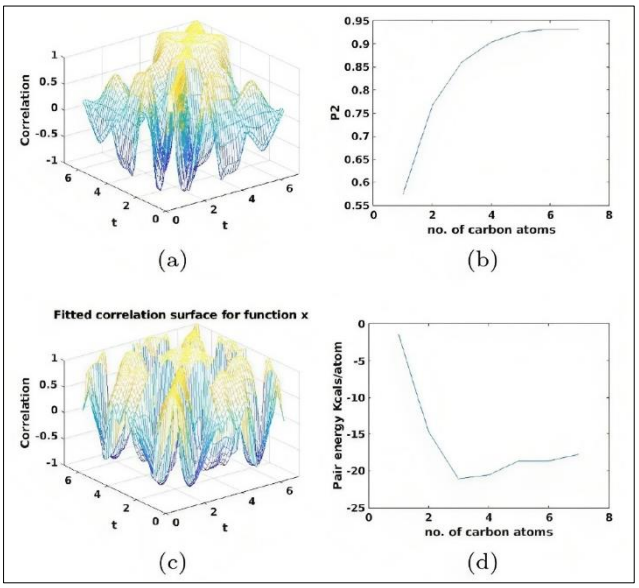

Figure 6. Correlation surface for orientational order parameter and air energy for homologous series **(a)** Correlation surface for P2; **(b)** Mean value of P2; **(c)** Correlation surface for pair energy; **(d)** mean value of pair energy (t=1 corresponds to p-azoxybenzene).

4. Conclusions

Based on the molecular dynamics study on the homologous series of alkyl-azoxy benzene compounds, several noteworthy outcomes have emerged: The stress-strain behavior across all series members remains linear, indicating consistent mechanical response under varying temperatures. At higher strain rates, an odd-even effect is observed in stress variations with the number of carbon atoms, highlighting structural influences on mechanical properties. Pair energy, bond energy, angle energy, and dihedral energy exhibit similar trends across all series members, suggesting uniformity in molecular interactions. For n=0, the pair correlation function indicates significant ordering in the first and second-order nearest neighbors, diminishing with increasing carbon atoms. The orientational order parameter P2 for n=0 aligns with Maier-Saupe criteria, ranging from 0.4 to 0.63, with higher values indicating a smectic phase presence. The presence or absence of a mesophase hinges on molecular structure, steric effects, and intermolecular interactions, showcasing the complex determinants of mesophase behavior. Heat capacity (Cv) increases with the number of carbon atoms, consistent with reasonably ordered phases, except for n=7, where the coiling of end chains leads to a decrease. Experimental observations of the odd-even effect in the orientational order parameter at transition temperatures support Maier-Saupe theory predictions, reinforcing correlations within the homologous series. Pair energy and Van der Waals potential variations with carbon atoms provide additional support for observed phenomena. Correlation analysis reveals strong relationships between order parameters and series members, indicating the influence of molecular interactions on mesophase characteristics.

In bioinformatics, liquid crystalline materials advance nucleic acid detection, label-free protein analysis, and real-time cellular monitoring, offering innovative solutions in molecular and cellular biology applications.

Funding

This research received no external funding.

Acknowledgments

The authors would like to thank all the potential reviewers for their valuable feedback.

Conflicts of Interest

The authors declare no conflict of interest.

References

1. Javadzadeh, M.; del Barrio, J.; Sánchez-Somolinos, C. Melt Electrowriting of Liquid Crystal Elastomer Scaffolds with Programmed Mechanical Response. *Adv. Mater.* **2023**, *35*, 2209244, https://doi.org/10.1002/adma.202209244.
2. Chen, M.; Gao, M.; Bai, L.; Zheng, H.; Qi, H.J.; Zhou, K. Recent Advances in 4D Printing of Liquid Crystal Elastomers. *Adv. Mater.* **2023**, *35*, 2209566, https://doi.org/10.1002/adma.202209566.
3. Chen, H.; Liu, Y.; Chen, M.; Jiang, T.; Zhang, L.; Yang, Z.; Yang, H. Research of Liquid-Crystal Materials for a High-Performance FFS-TFT Display. *Molecules* **2023**, *28*, 754, https://doi.org/10.3390/molecules28020754.
4. Li, J.; Xu, S.; Li, Y.; Wan, L.; Wei, G.; Jiang, T.; Li, Z.; Yang, Y. Suppressing the self-discharge of MXene-based supercapacitors by liquid crystal additive. *Nano Energy* **2023**, *115*, 108754, https://doi.org/10.1016/j.nanoen.2023.108754.
5. Mitov, M. Liquid-Crystal Science from 1888 to 1922: Building a Revolution. *ChemPhysChem* **2014**, *15*, 1245-1250, https://doi.org/10.1002/cphc.201301064.
6. Matharu, A.S.; Wu, Y. Liquid Crystal Displays: from Devices to Recycling. In Electronic Waste Management, Goosey, M., Stevens, G., Herman, H., Baird, P., Holmes, I., Kell, D., Kellner, R., Butler, S., Shayler, M., Holloway, L., et al., Eds.; The Royal Society of Chemistry, **2009**; 180-211, https://doi.org/10.1039/9781847559197-00180.
7. Leal-Junior, A.; Soares, M.S.; de Almeida, P.M.; Marques, C. Cholesteric Liquid Crystals Sensors Based on Nanocellulose Derivatives for Improvement of Quality of Human Life: A Review. *Adv. Sens. Res.* **2023**, *2*, 2300022, https://doi.org/10.1002/adsr.202300022.
8. Concellón, A. Liquid Crystal Emulsions: A Versatile Platform for Photonics, Sensing, and Active Matter. *Angew. Chem., Int. Ed.* **2023**, *62*, e202308857, https://doi.org/10.1002/anie.202308857.
9. Prakash, J.; Parveen, A.; Mishra, Y.K.; Kaushik, A. Nanotechnology-assisted liquid crystals-based biosensors: Towards fundamental to advanced applications. *Biosens Bioelectron.* **2020**, *168*, 112562, https://doi.org/10.1016/j.bios.2020.112562.
10. Qin, J.; Ning, S.; Xu, J.; Zeng, J.; He, Z.; Luo, L.; Hu, F.; Li, Y.; Fujita, T.; Wei, Y. Separation and recovery of indium in hazardous liquid crystal display treatment by a novel silica adsorbent: Study on adsorption mechanism and process design. *J. Clean. Prod.* **2023**, *425*, 138999, https://doi.org/10.1016/j.jclepro.2023.138999.
11. Prakash, J.; Varshney, D.; Chauhan, S.; Kaushik, A.; Mishra, Y.K. Progress in radiations induced engineering of liquid crystals properties for high-performance applications. *Phys. Rep.* **2023**, *1015*, 1-23, https://doi.org/10.1016/j.physrep.2023.03.003.
12. Luckhurst, G.R. Liquid crystals: a chemical physicist's view. *Liq. Cryst.* **2005**, *32*, 1335-1364, https://doi.org/10.1080/02678290500423128.
13. de Pablo, J.J.; Yan, Q.; Escobedo, F.A. SIMULATION OF PHASE TRANSITIONS IN FLUIDS. *Annu. Rev. Phys. Chem.* **1999**, *50*, 377-411, https://doi.org/10.1146/annurev.physchem.50.1.377.

14. Allen, M.P.; Frenkel, D. Calculation of liquid-crystal Frank constants by computer simulation. *Phys. Rev. A* **1988**, *37*, 1813, https://doi.org/10.1103/PhysRevA.37.1813.
15. Humpert, A.; Brown, S.F.; Allen, M.P. Molecular simulations of entangled defect structures around nanoparticles in nematic liquid crystals. *Liq. Cryst.* **2018**, *45*, 59-69, https://doi.org/10.1080/02678292.2017.1295478.
16. Dierking, I. Nanoscience with liquid crystals. *Liq. Cryst. Today* **2017**, *26*, 63-65, https://doi.org/10.1080/1358314x.2017.1359140.
17. Priscilla, P.; Malik, P.; Supreet; Kumar, A.; Castagna, R.; Singh, G. Recent advances and future perspectives on nanoparticles-controlled alignment of liquid crystals for displays and other photonic devices. *Crit. Rev. Solid State Mater. Sci.* **2023**, *48*, 57-92, https://doi.org/10.1080/10408436.2022.2027226.
18. Bisoyi, H.K.; Li, Q. Liquid Crystals: Versatile Self-Organized Smart Soft Materials. *Chem. Rev.* **2022**, *122*, 4887-4926, https://doi.org/10.1021/acs.chemrev.1c00761.
19. Prakash, J.; Khan, S.; Chauhan, S.; Biradar, A.M. Metal oxide-nanoparticles and liquid crystal composites: A review of recent progress. *J. Mol. Liq.* **2020**, *297*, 112052, https://doi.org/10.1016/j.molliq.2019.112052.
20. Urban, S.; Czub, J.; Gestblom, B. Comparison of Dielectric Properties of Three Alkyl and Alkoxy Azoxybenzenes (*n*AOBs and *n*OAOBs, *n* = 5,6,7) in the Isotropic and Liquid Crystalline Phases. *Z. Naturforsch. A.* **2004**, *59*, 674-682, https://doi.org/10.1515/zna-2004-1009.
21. Andrews, M.A.; Schroeder, D.C.; Schroeder, J.P. Liquid crystals : III. 4,4′-di-*n*-alkoxyazoxybenzenes and their mixtures as stationary liquid phases in gas—liquid chromatography. *J. Chromatogr. A* **1972**, *71*, 233-242, https://doi.org/10.1016/S0021-9673(01)80681-6.
22. Capaldi, F.M.; Boyce, M.C.; Rutledge, G.C. Molecular response of a glassy polymer to active deformation. *Polymer* **2004**, *45*, 1391-1399, https://doi.org/10.1016/j.polymer.2003.07.011.
23. Capaldi, F.M.; Boyce, M.C.; Rutledge, G.C. Enhanced Mobility Accompanies the Active Deformation of a Glassy Amorphous Polymer. *Phys. Rev. Lett.* **2002**, *89*, 175505, https://doi.org/10.1103/PhysRevLett.89.175505.
24. Hossain, D.; Tschopp, M.A.; Ward, D.K.; Bouvard, J.L.; Wang, P.; Horstemeyer, M.F Molecular dynamics simulations of deformation mechanisms of amorphous polyethylene. *Polymer* **2010**, *51*, 6071-6083, https://doi.org/10.1016/j.polymer.2010.10.009.
25. Dodda, L.S.; Vilseck, J.Z.; Tirado-Rives, J.; Jorgensen, W.L. 1.14*CM1A-LBCC: Localized Bond-Charge Corrected CM1A Charges for Condensed-Phase Simulations. *J. Phys. Chem. B* **2017**, *121*, 3864-3870, https://doi.org/10.1021/acs.jpcb.7b00272.
26. Dodda, L.S.; de Vaca, I.C.; Tirado-Rives, J.; Jorgensen, W.L. LigParGen web server: an automatic OPLS-AA parameter generator for organic ligands. *Nucleic Acids Res.* **2017**, *45*, W331-W336, https://doi.org/10.1093/nar/gkx312.
27. Singh, H.; Raja, A.; Prakash, A.; Medhi, B. Gmx_qk: An Automated Protein/Protein-Ligand Complex Simulation Workflow Bridged to MM/PBSA, Based on Gromacs and Zenity-Dependent GUI for Beginners in MD Simulation Study. *J. Chem. Inf. Model* **2023**, *63*, 2603-2608, https://doi.org/10.1021/acs.jcim.3c00341.
28. Panwar, P.; Yang, Q.; Martini, A. PyL3dMD: Python LAMMPS 3D molecular descriptors package. *J. Cheminform.* **2023**, *15*, 69, https://doi.org/10.1186/s13321-023-00737-5.
29. Polymer Data Handbook, 2nd Ed. *J. Am. Chem. Soc.* **2009**, *131*, 16330, https://doi.org/10.1021/ja907879q.
30. Kahn, F.J. The molecular physics of liquid-crystal devices. *Phys. Today* **1982**, *35*, 67-74, https://doi.org/10.1063/1.2915096.
31. Tabe, Y.; Urayama, K.; Matsuyama, A.; Yamamoto, J.; Yoneya, M. Physics of Liquid Crystals. In The Liquid Crystal Display Story: 50 Years of Liquid Crystal R&D that lead The Way to the Future, Koide, N., Ed.; Springer Japan, Tokyo, **2014**; 301-356, https://doi.org/10.1007/978-4-431-54859-1_10.
32. Fumeron, S.; Berche, B. Introduction to topological defects: from liquid crystals to particle physics. *Eur. Phys. J.: Spec. Top.* **2023**, *232*, 1813-1833, https://doi.org/10.1140/epjs/s11734-023-00803-x.
33. Maier, W.; Saupe, A. A SIMPLE MOLECULAR THEORY OF THE NEMATIC LIQUID-CRYSTALLINE STATE: Physical Chemistry and Physics Institute of the University of Freiburg i. Br. In Crystals That Flow; CRC Press, **1959**; 402-421.
34. Luckhurst, G.R.; Zannoni, C. Why is the Maier–Saupe theory of nematic liquid crystals so successful?. *Nature* **1977**, *267*, 412-414, https://doi.org/10.1038/267412b0.

35. Urs, T.G.K.; Bharath, K.; Yallappa, S.; Rudrappa, S. Functional data analysis techniques for the study of structural parameters in polymer composites. *J. Appl. Cryst.* **2016**, *49*, 594-605, https://doi.org/10.1107/S1600576716003113.
36. Grobben, A.H. Liquid crystalline azoxybenzene compounds. U.S. Patent 3,907,768, issued September 23, 1975, https://patents.google.com/patent/US3907768A/en.
37. Hegde, V.N.; Jyothi, K.R.; Bhagya, K.R.; Lumbini, J.; Somashekar, R.; Nagabhushana, H.; Manju, V.V. Structural, morphological and mechanical properties of Dy^{3+} doped $Sr_2MgSi_2O_7$ nanocomposites. *J. Solid State Chem.* **2022**, *315*, 123501, https://doi.org/10.1016/j.jssc.2022.123501.